UCRL 3173

UNIVERSITY OF
CALIFORNIA

Radiation
Laboratory

BUBBLE CHAMBER PRESSURE GAGE

BERKELEY, CALIFORNIA

DISCLAIMER

1

UCRL-3173
Instrumentation Distribution

UNIVERSITY OF CALIFORNIA
Radiation Laboratory
Berkeley, California
Contract No. W-7405-eng-48

BUBBLE CHAMBER PRESSURE GAGE

William I. Linlor and Quentin A. Kerns

October 20, 1955

Printed for the U.S. Atomic Energy Commission

BUBBLE CHAMBER PRESSURE GAGE

Contents

BUBBLE CHAMBER PRESSURE GAGE

William I. Linlor and Quentin A. Kerns

Radiation Laboratory, Physics Department
University of California, Berkeley, California

October 20, 1955

ABSTRACT

A description is given of the mechanical gage and electrical circuit employed in measuring pressure pulses in a liquid hydrogen bubble chamber.

The pressure pulse produces a deflection of a diaphragm which acts as one electrode of a capacitor. The change in capacitance is measured in a circuit by measuring the difference in reflected pulses from two terminations at the ends of similar cables fed by a common source; one of the terminations is the pressure-measuring capacitor, the other is a comparison capacitor.

BUBBLE CHAMBER PRESSURE GAGE

William I. Linlor and Quentin Kerns

Radiation Laboratory, Physics Department
University of California, Berkeley, California

October 20, 1955

INTRODUCTION

This report is a description of a pressure gage which was designed specifically for use in a liquid-hydrogen bubble chamber.[1,2]

Two basic requirements were specified for the gage:

(a) Immersion in liquid hydrogen. This implied that the unit would not be accessible for adjustment, must operate at a temperature of about -260°C, and would necessarily have a connecting lead at least a foot long.

(b) Response time of 10^{-4} second or less. This was necessary in order to measure details in a pressure pulse which was believed to range from about 100 pounds per square inch to atmospheric pressure in a millisecond.

After some preliminary experiments and literature searching, it was decided to measure the pressure change by the displacement of a diaphragm which acted as an element of a capacitive cell.

The advantages of this arrangement seemed to be the excellent frequency response of a pressure-deflected plate, and the avoidance of thermoelectric effects, which could present problems in a metallic circuit.

A serious disadvantage was the fact that the capacitance of the unit would necessarily be of the order of a micromicrofarad, and so the pressure-produced change in capacitance would be even less. (A deflection of the center of the plate amounting to a few wave lengths of red light is produced by the smallest pressure change that was to be measured by the corresponding capacitance change.)

The basic problem, therefore, was to develop an electrical circuit that could measure a small transient capacitance change in the presence of much larger parallel cable capacitance.

Another problem was the design of a suitable capacitive pressure pick-up ("transducer"). We were assisted in this by a published description of "miniature pressure cells",[3] and by consultation with Taft Wrathall and Grant Coons, of the Ames Aeronautical Laboratory at Moffett Field, California. Only minor modifications of their cell design were needed to adapt it to the bubble-chamber application.

In the following material we describe the present version of the UCRL pressure-measuring system. Operating experience from February 1955 to date has been sufficiently trouble-free so that no compelling motivation exists for further development at the present time.

Undoubtedly there are many potential uses for the gage, but we restrict the following material to a description and discussion of the bubble-chamber application.

DESCRIPTION OF PRESSURE CELL

A sectional drawing of the pressure cell is given in Fig. 1. The components of the unit are:

a. The external shell or body, (Fig. 2). This is essentially a cylinder one inch long and one inch in outside diameter, machined out of solid stainless steel. The diaphragm at one end is 0.025 inch thick. To preserve its elastic deflecting property, the diaphragm must be machined slowly when the final thickness is approached, and subsequently it should not be subjected to loading greater than the pressure to be measured.

b. The inner electrode, (Fig. 3). This is also machined out of stainless steel. As is evident from the assembly drawing, this electrode is spaced (by machining its surface) 0.003 inch from the diaphragm. Adjustments in the field have been carried out by shims between the electrode and the shell or the spacer and the shell. The hole in the inner electrode has had to be soldered shut at the diaphragm end to avoid entrance of small metal chips when the "microdot" connector is inserted.

c. Spacer (Fig. 4). This is a canvas-base bakelite spacer. Its properties do not seem to be critical in any sense.

d. External connector (Fig. 5). This is an adaptor for a commercially available "microdot" connector.

e. Retaining nuts (Figs. 6a, 6b). These are machined out of stainless steel.

The resonant frequency of the diaphragm can be approximately calculated by standard thin-shell theory. Obviously an exact analysis is difficult because the diaphragm in effect is "clamped" by the external cylinder. Even though the metal is presumed to be stress-free at room temperature, it is unquestionably stressed internally at liquid hydrogen temperatures.

The deflection sensitivity (i.e., the deflection per unit pressure change) is also dependent on the temperature. The difference in sensitivity between room and liquid-hydrogen temperatures affords a basis for estimating the resonant-frequency change due to temperature. To see this, one can think of the diaphragm as a lumped mass having an associated spring constant, the latter being inversely proportional to the deflection sensitivity. The resonant frequency of the lumped system is proportional to the square root of the spring constant.

The resonant frequency of a sample cell having a diaphragm 0.050 inch thick was measured at room temperature; it was approximately 30 kc. The cell was not attached to a bubble-chamber wall; it was a movable unit.

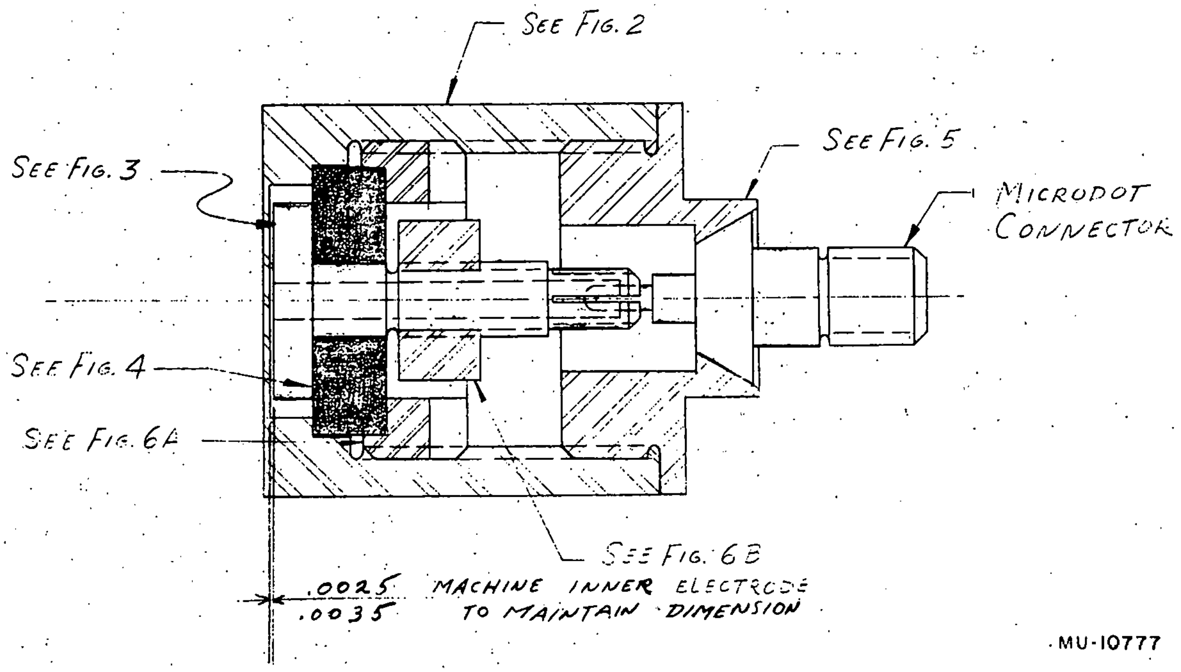

MU-10777

Fig. 1. Sectional drawing of the pressure cell.

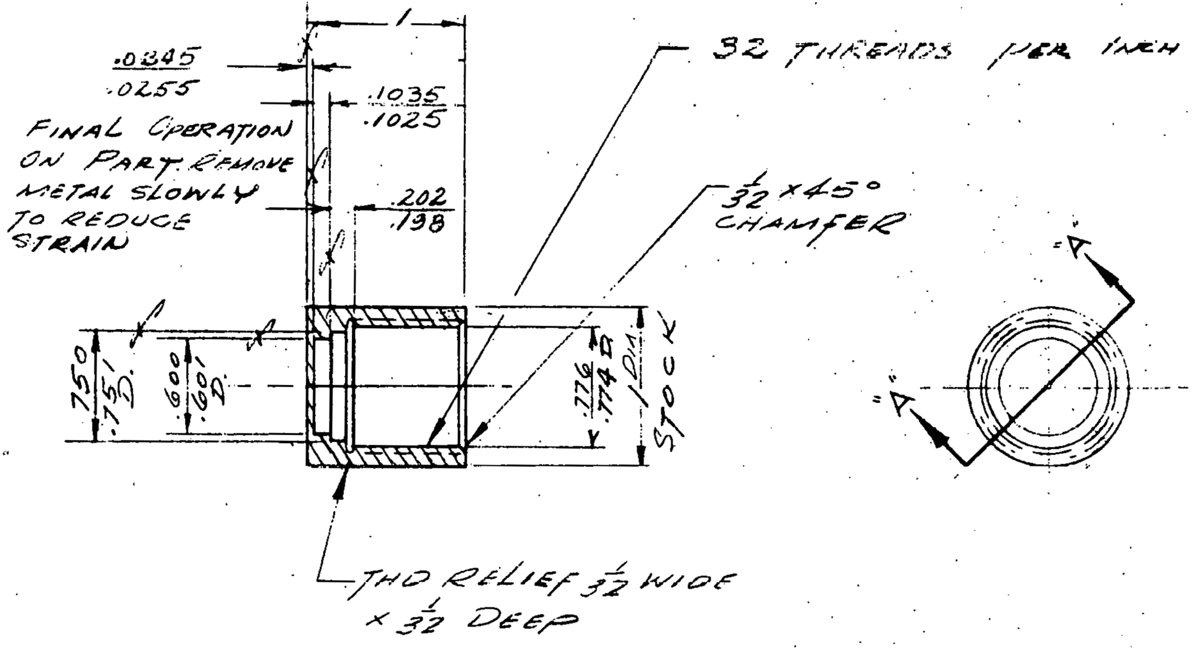

MU-10776

Fig. 2. External shell of pressure cell.

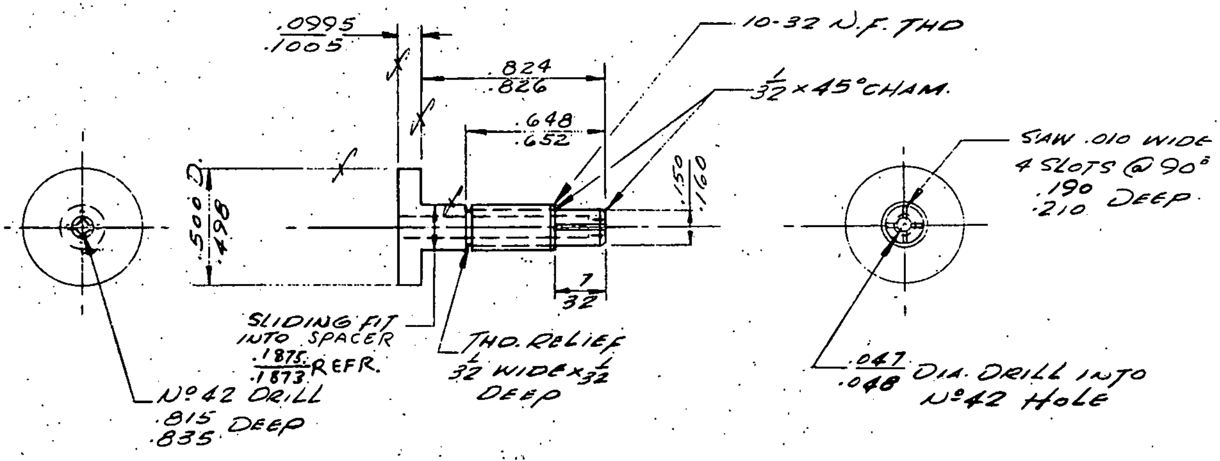

MU-10775

Fig. 3. The inner electrode.

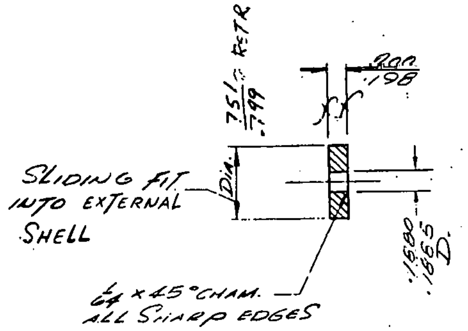

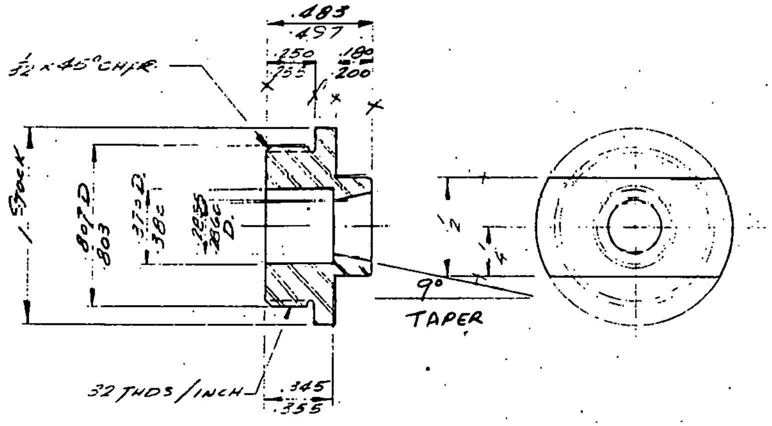

MU-10774

Fig. 4. Spacer. Fig. 5. External connector.

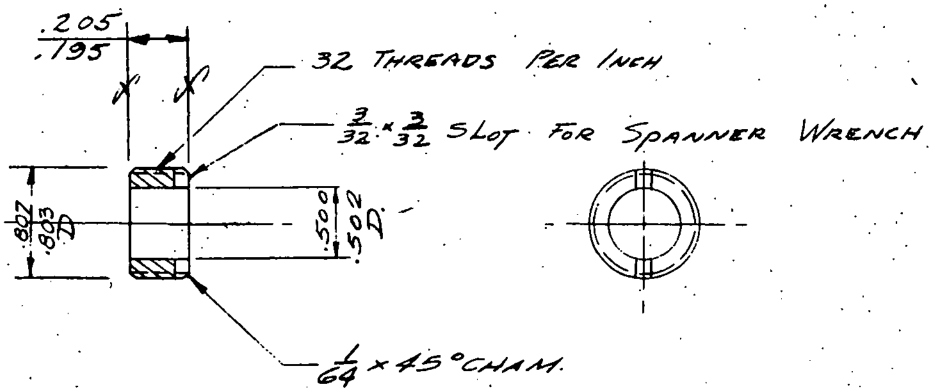

6 A

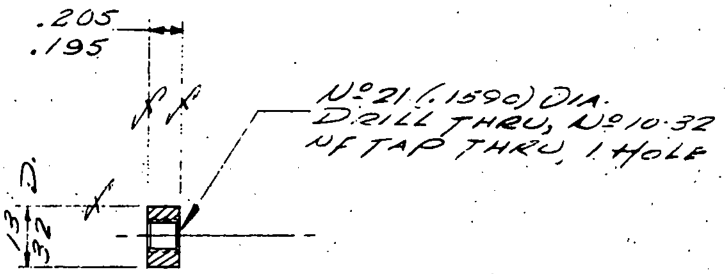

6 B

MU-10773

Fig. 6a. Retaining nut.

Fig. 6b. Inner plate nut.

In practice, the shell body 7N1662 (Fig. 1) is made a part of the chamber wall by soldering, so that the diaphragm is in contact with the liquid hydrogen. Such constraint also affects the resonant frequency, increasing it in general.

GENERAL DESCRIPTION OF ELECTRICAL CIRCUIT

The basic electrical circuit is shown in Fig. 7, a block diagram of the actual circuit in Fig. 8. The detailed electrical circuit is described in the next section.

Referring to Fig. 7, which represents an idealization of the method, we assume that a sine-wave positive pulse S (about 10^{-8} second wide and 100 volts high) is generated by the pulser and delivered to a transformer. At the output of the center-tapped transformer, symmetrical positive and negative pulses S_1 and S_2 appear. If we choose cable No. 1 and cable No. 2 to have the same surge impedance, the circuit is symmetrical about the point CT and none of the transmitted pulse is presented to the crystal diode.

The transmitted pulses S_1 and S_2 travel down Cables 1 and 2 to encounter the terminations. These terminations may take a variety of forms; for simplicity we select them to be the pressure-measuring capacitance cell C_1 and an adjustable comparison capacitor C_2. From the terminations, reflected pulses r_1 and r_2 travel back along the cables to the transformer, the sum $r_a = r_1 + r_2$ appearing at the point CT. Capacitor C_a is charged through the diode to a voltage somewhat below the positive peak of r_a. The charging time is of the order of 10^{-8} sec, whereas the discharge time, essentially C_aR_a, is adjusted to about 5×10^{-7} second. Such pulse stretching permits the use of moderate band-width circuitry in the subsequent determination of the pulse voltage on C_a.

Evidently, in a completely symmetrical system the sum of r_1 and r_2 is zero. If the capacitance C_1 then changes as the result of an applied pressure, the sum $r_a = r_1 + r_2$ is no longer zero, but is a function of the applied pressure. If we regard C_1, the capacitance of the pressure cell, as the sum of a fixed component C_0 and a pressure-related component ΔC, the ratio $\frac{\Delta C}{C_0}$ is the fractional change in capacitance to be measured. The range of values $\frac{\Delta C}{C_0}$ from 0.00 to 0.01 may represent a total pressure range.

Before proceeding to the more complicated circuits, let us discuss some of the features of the system.

Cable Properties

Coaxial cable is the information channel between the measuring circuit and the pressure cell. For the present application, physical cable departs from the ideal transmission line in two general respects: first, existing cable attenuates and disperses pulses in transit, and second, the cable link exhibits impedance variations along the path as a result of joints, interconnecting plugs,

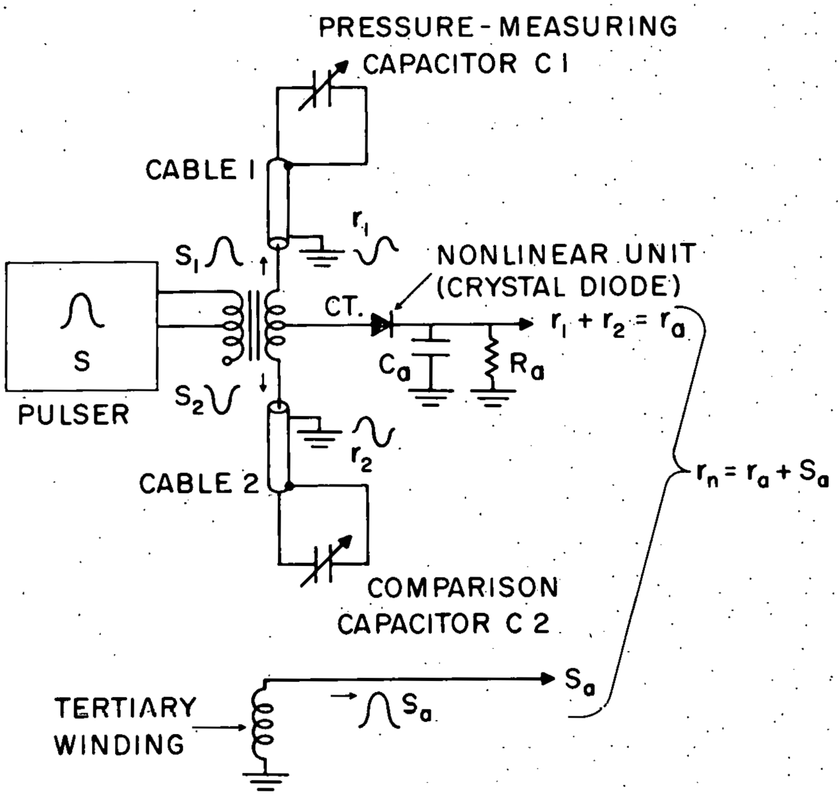

MU-10772

Fig. 7. Basic electrical circuit for bubble-chamber pressure gage, idealized.

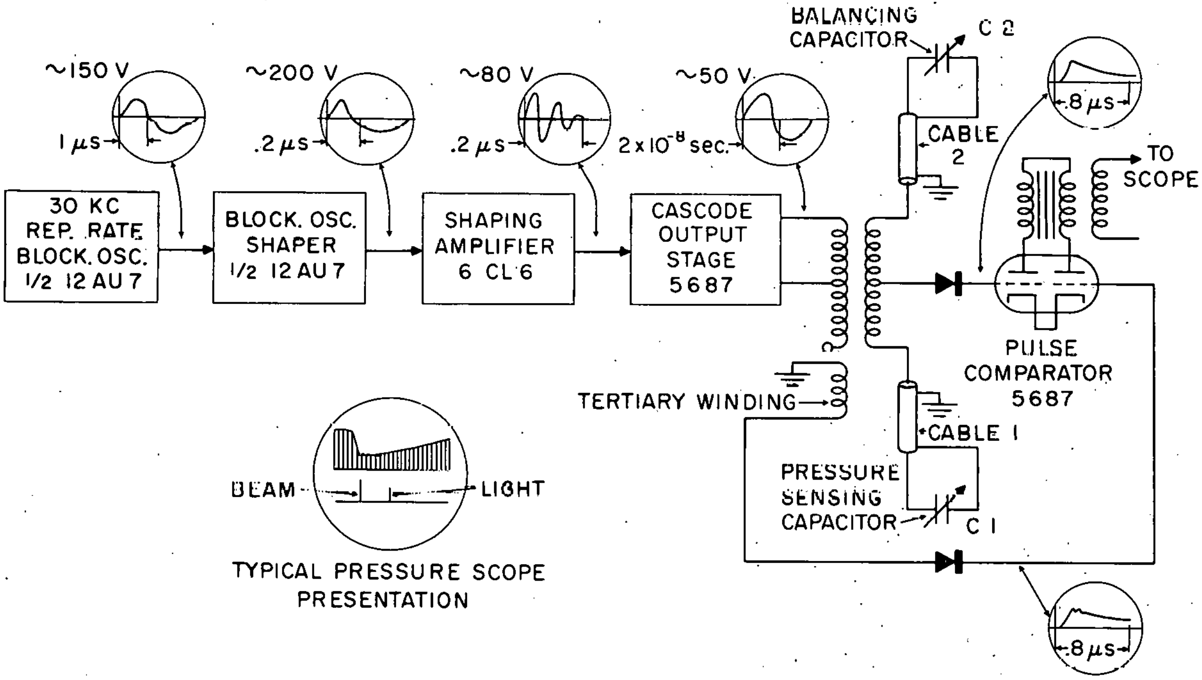

Fig. 8. Block diagram of actual circuit for pressure gage.

normal cable tolerances, etc.

The attenuation and dispersion are governed by the cable used. In a 300-foot round trip in RG 7/U, for example, a pulse such as S is reduced to about half amplitude and lengthened a few percent. Distortion of this order is not significant in the over-all performance, since the effect for a particular cable is absorbed in the output-vs-pressure calibration. Applications requiring the pressure cell to be more than a few hundred feet away call for electrically better cable. Phelps-Dodge 1-1/8-inch Styroflex would be satisfactory for distances of a mile or so.

Impedance variations along the cable give rise to a background of undesired reflections. In general, the signal appearing at point CT in Fig. 7 is not a single pulse but a train of pulses, the last of which is the desired pressure-sensitive reflection from C_1. It was elected to discriminate in favor of the desired pulse on the basis of amplitude. Since the crystal diode-capacitor combination is not an absolute peak-reading device, the desired pulse should be several times as high as the background pulses. The reliable reading of a small pressure variation thus requires a low background level.

Background can be reduced by introducing at appropriate places into cable No. 2 the same joints, plugs, etc., as are necessary in cable No. 1. One may even use a succession of different cable types for Cable 1, such as 10 feet of RG 63/U, followed by 2 feet of RG 7/U, etc., provided Cable 2 is assembled correspondingly.

The care required in cable matching in order that background not be a limitation may be estimated from considerations of the pulse width. Pulse energy at any instant is confined to about 10 feet of free space or about eight feet of RG 7/U cable, given a pulse width at half amplitude of 1×10^{-8} sec. A time difference of 0.01 pulse width, or about 1 inch of cable, represents a good working tolerance.

It may be that the electrical cable length is not proportional to the physical length. For example, a variation in the dielectric constants of Cables 1 and 2 may make the following adjustment necessary: with no termination on the cables, one observes the signal sum $r_1 + r_2$. Using pliers or tinsnips, one adjusts the relative length judiciously until $r_1 + r_2$ is minimum. (In practice, one centimeter difference gives rise to a relatively large r_a.)

A comment is appropriate about the length of cable required to be at low temperature. It was found experimentally that a teflon-dielectric cable did not exhibit too much temperature effect, whereas some other dielectrics did. In the latter case, a balance of electrical cable lengths was difficult to obtain.

In summary, we see that cable lengths from about a foot to a few thousand feet may be employed. Any residual discontinuities in the cable system should be several times smaller than that afforded by C_1.

Adjustment

Because the capacitance of the pressure cell C_1 changes with temperature, some means must be provided for suitable adjustment in the circuit. The comparison capacitor C_2 is available for this adjustment, since a positive increment in C_2 has essentially the same circuit effect as a negative increment in C_1.

Normally, C_2 is set to a value slightly different from that of C_1 in order to keep the desired pulse above the background level. The effect on the sum $r_1 + r_2$ of a variation in C_2 is shown in Fig. 9.

At $C_1 = C_2$, the pressure-sensitive pulse has disappeared, while the level $r_1 + r_2$ is supported by the residual background. (The dotted lines, curve b, show the hypothetical case of perfect symmetry, giving zero background.)

Since the slope of the curve in Fig. 9 is proportional to the sensitivity, one should deliberately set $C_1 \neq C_2$, in a region where the slope is approximately a straight line, in order to get suitable sensitivity as well as linear relation between pressure changes and signal output. Differences in cable length within the allowed tolerance may be compensated by the setting of C_2.

Another reason for setting $C_2 \neq C_1$ arises from the conductivity characteristic of the rectifier. If $r_a = r_1 + r_2$ has a steady-state positive value, the incremental conductivity of the crystal diode for a small change in r_a is greater than it would be if $r_a = 0$ nominally. In the present circuit the $C_1 - C_2$ unbalance is deliberately made relatively large. The steady-state positive signal is then bucked out with a negative signal obtained from a similar rectifier operating on a constant amplitude pulse S_a from a tertiary winding on the transformer. S_a is of course not simultaneous in time with r_a, preceding r_a by the round-trip transit time in cable No. 1. The pulse stretching of both R_a and S_a permits them to overlap and essentially buck out in the narrow band-width circuits following.

Calibration

The pressure-vs-output calibration can be obtained by noting the output for various constant pressures. The limiting frequency response seems to be that of the diaphragm.

If one neglects the effects of the liquid hydrogen because of its low density compared to steel, the constant-pressure calibration seems to be accurate to within a few percent up to a frequency of 1/4 of the diaphragm resonant frequency, according to standard oscillation theory. In terms of numbers, let us assume that the natural resonant frequency of the (clamped) diaphragm at liquid-hydrogen temperature is 40 kc. A pressure pulse of one millisecond duration could be measured by the gage in 0.1-millisecond intervals. Such readings would not be in error by more than a few percent, as far as diaphragm response characteristics are concerned, if one used the constant-pressure calibration.

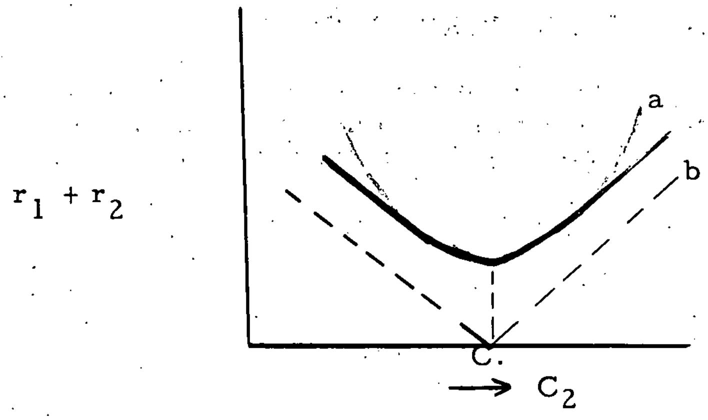

Fig. 9. Relation between pulse $r_1 + r_2$ and capacitance C_2.

Display

Oscilloscope display of the pulse is an obvious step. Triggering the scope and photographing the sweep present no unusual problems to those working in the field.

Block Diagram

A block diagram of the circuit is shown in Fig. 8. This is self-explanatory. The reason for selecting a 30-kc repetition rate for the pulse generator is that this would allow observation of pressure values at 1/30,000-second intervals. The frequency-response characteristic of the diaphragm may cloud the pressure response at higher repetition rates.

Since each pulse reading, as delivered to the oscilloscope, is about a microsecond wide, the display consists of a series of pulses each 10^{-6} second wide, separated by 3×10^{-5} second. For a sweep which lasts, say, 10 milliseconds, there would be 300 pulses. The appearance is shown schematically in the "Typical Pressure Scope Presentation" of Fig. 8.

DETAILED ELECTRICAL CIRCUIT

The details of the electrical circuit are shown in Figs. 10a and 10b. (This division into two portions is necessary for clarity in the report-reproduced drawings. The corresponding UCRL drawing number is 4V4324.)

A few comments about the circuit may be helpful.

The plug PG-3 is available in order to observe the "initial" pulses on a suitably fast scope. Plug PG-4, labeled X cable, is the comparison branch No. 2 of Fig. 1. Plug PG-5 is the pressure-measuring branch No. 1 of Fig. 7.

The impedance level of all the coaxial cables is 125 ohms. Doubly shielded RG-63/U (Amphenol 24-406) has been used with satisfactory results. Both shields are grounded at both ends. The length of each cable is about 50 feet.

A trigger pulse is available on plug PG-2, polarity positive.

The sensitivity of the over-all device to pressure changes is related to the initial pulse duration. One might consider setting the cable impedance Z_0 equal to the pressure cell reactance X_{C_1} at a frequency ω corresponding to the single cycle pulse. This would give $Z_0 = X_{C_1} = \frac{1}{\omega C_1}$ and therefore the period of one cycle $T = \frac{2\pi}{\omega} = 2\pi Z_0 C_1$. Figure 11 shows the relative sensitivity for various experimental ratios $\frac{T}{Z_0 C_1}$, where sensitivity is defined as $\frac{\Delta r_a}{S} / \frac{\Delta C}{C_1}$,

where Δr_a = amplitude increment of reflected pulse at CT,

S = amplitude of initial signal,

ΔC = pressure-produced capacitance change,

$C_1 \approx C_0$ = fixed capacitance of pressure cell.

Figure 11 shows a broad maximum near $\frac{T}{Z_0 C_1} = 10$ for the circuit of Fig. 7. The general behavior is clear. If the pulse width T is gradually decreased from the optimum, eventually it becomes less than the time constant $Z_0 C_1$. The pulse then fails to charge the capacitance C_1 appreciably, hence is almost totally reflected. Small variations in C_1 at this point produce negligible change in the reflection. Thus the sensitivity to pressure vanishes for infinitely narrow pulses, which see only a short circuit at the pressure cell. For very long pulses, on the other hand, the charging current to C_1 is small, hence the pressure-sensitive voltage pulses are again small. For the cell described here, T is set at about 2×10^{-8} sec, Z_0 is 125 ohms,

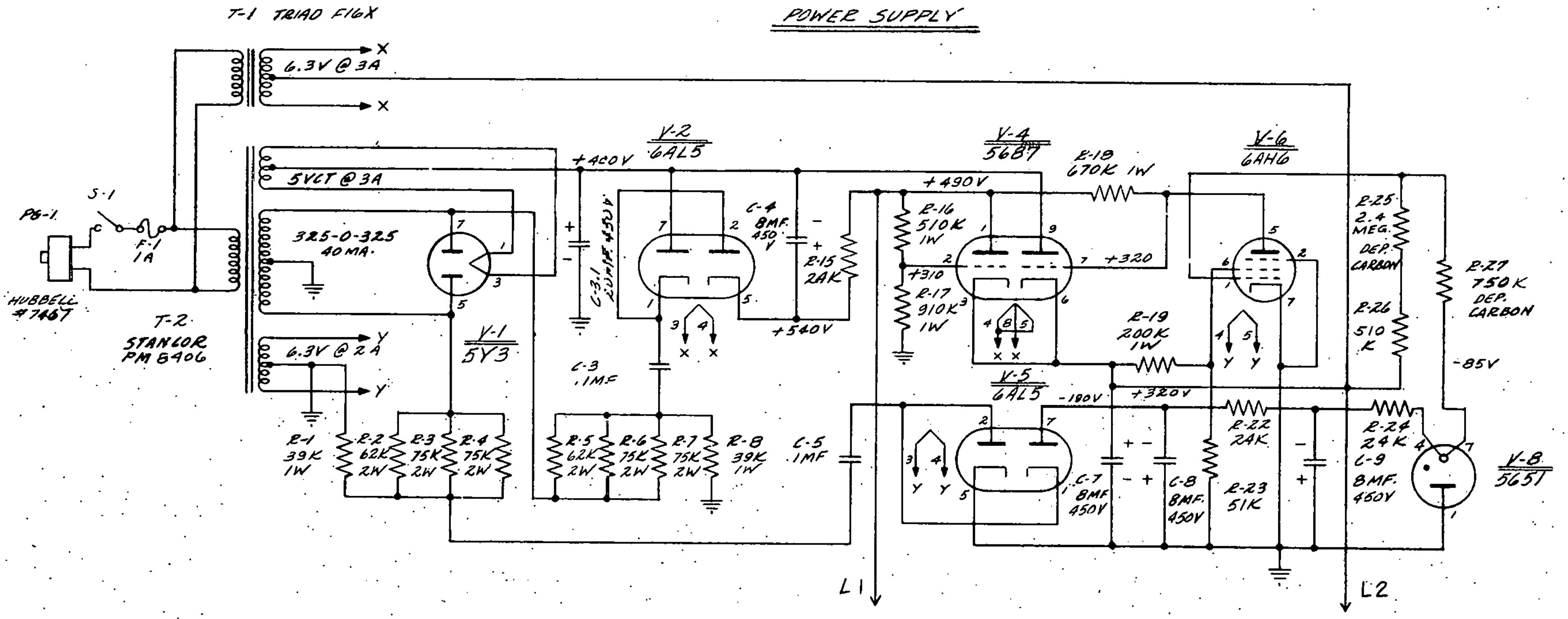

ZN-1456

Fig. 10a. Details of the power supply.

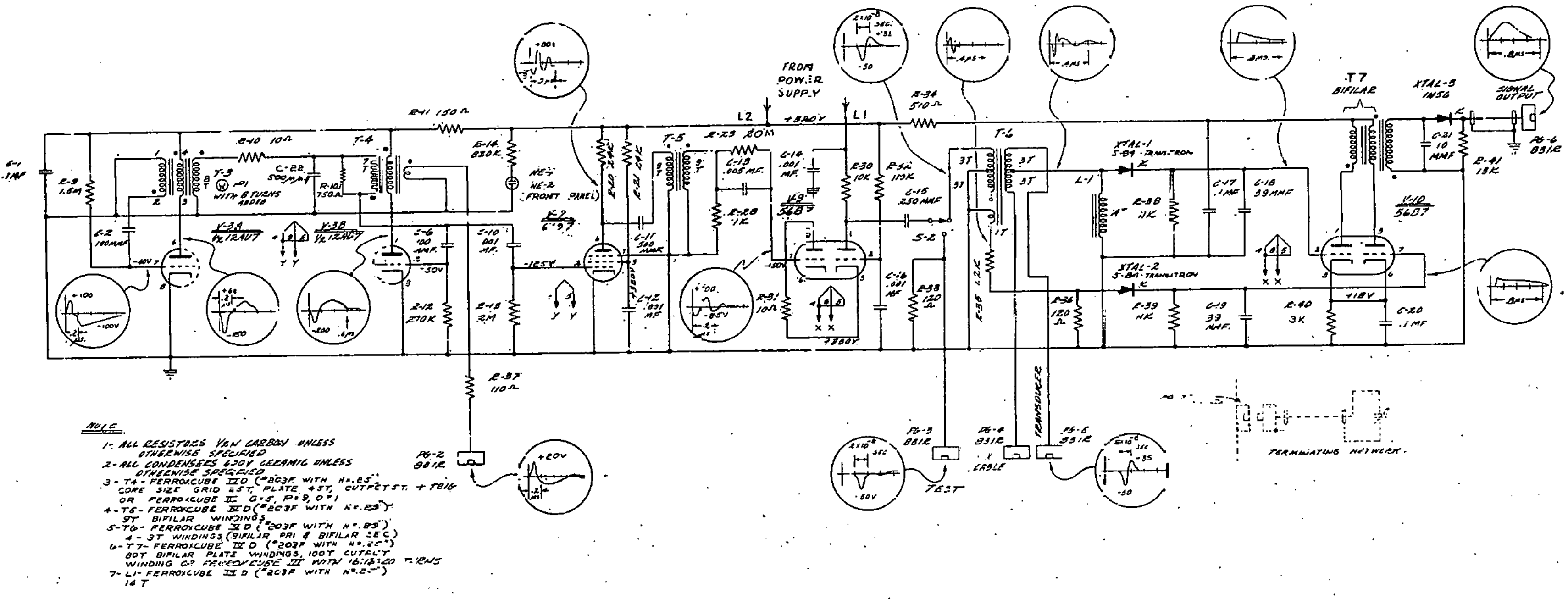

ZN-1457

Fig. 10b. Details of the electrical circuit.

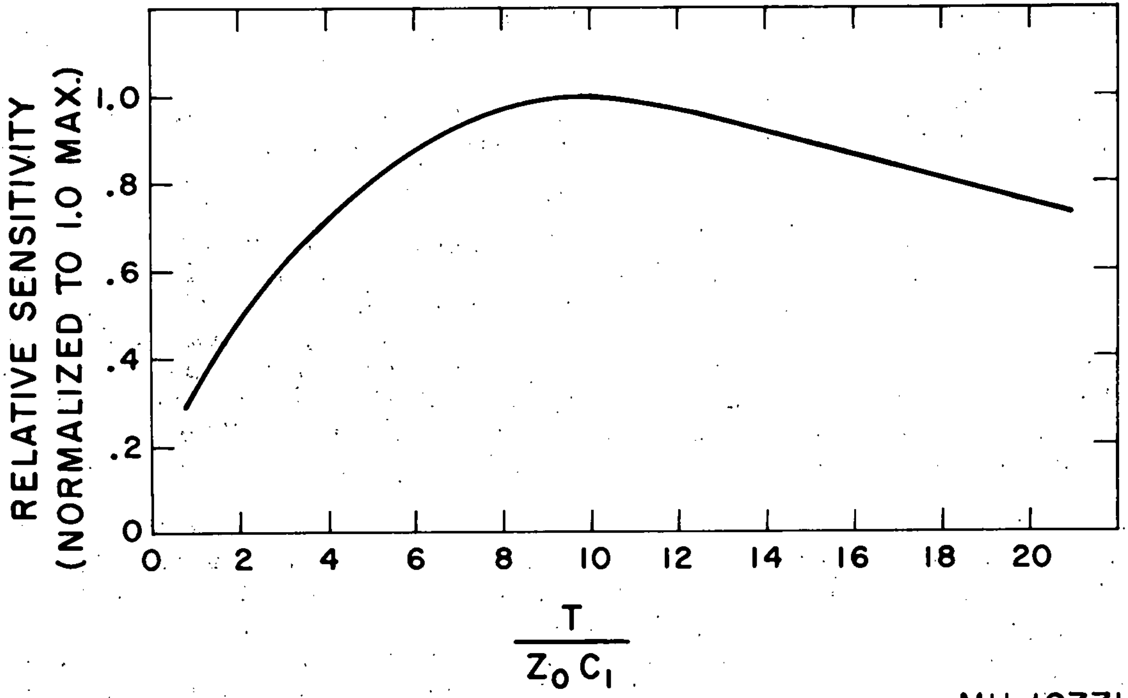

MU-10771

Fig. 11. Relation between sensitivity and pulse length.

and C_1 about 1.5×10^{-11} farad. Then

$$\frac{T}{Z_0 C_1} = \frac{2 \times 10^{-8}}{125 \times 1.5 \times 10^{-11}} \approx 11.$$

Now, considering the circuit in more detail, we note that the blocking oscillator (1/2 12AU7) generates a positive pulse of about one-microsecond duration, repetition frequency about 30 kc. The pulse length is decreased to about 0.2 microsecond in the following blocking oscillator (1/2 12AU7) and then is fed into a shaping amplifier (6CL6), which is replaced by 6197-type in later versions of the circuit. The grid of the latter is biased sufficiently negative by grid rectification so that a pulse of plate current is passed only at the tip of the incoming pulse. Transformer T-5 produces a positive-going damped pulse which is fed to the cascode output stage. The cascode stage (5687) is sensitive only to the first positive pulse of the ringing because of the self-bias developed. The result is a pulse about 50 volts negative going to 35 volts positive in about 10^{-8} second. This is the desired "initial" pulse needed for the measuring circuit.

Switch S-2 permits checking the initial pulse on a suitable fast scope, from plug PG-3. As shown on the drawing, the switch is in the pressure-measurement position.

The pulse just described is fed into one half of the primary of the output transformer (T-6); the other half (three turns) is left floating to achieve electrostatic balance between primary and secondary. The necessary pulse symmetry in the transformer is achieved by winding the two halves of each center-tapped winding in the form of a three-turn twisted pair, so that each half of the winding takes a similar path about the toroidal core. The pulses from the secondary are thus alike except for polarity. These are the pulses delivered to the cables No. 1 and No. 2 at plugs PG-5 and PG-4 respectively.

The reflected pulses from the terminations are added in the transformer secondary, and the algebraic sum is fed through a crystal diode (XTAL-1) into an integrating capacitor (C-18). The voltage appearing on the capacitor is fed to the grid of one triode of the pulse-comparator tube (5687). A reference bucking signal is fed to the other grid of the comparator tube through a crystal diode (XTAL-2) by the single-turn tertiary winding of the transformer (T-6). The pulse-comparator tube thus acts as a difference amplifier.

The outputs of the two triodes of the pulse-comparator tube appear on push-pull primary windings of a transformer (T-7) in the plate circuit. The output of the secondary winding of this transformer is the desired signal, which is produced by a pressure change in the bubble chamber, and appears at plug PG-6.

The crystal diodes and associated RC circuits serve to lengthen the output of the secondary winding, so as to permit use of a relatively "slow" and therefore inexpensive amplification and oscilloscope equipment.

A dual-beam oscilloscope has been used, which shows pressure variation on the upper sweep, and related events regarding the bubble chamber on the lower sweep. These related events are "instant" of beam-pulse from the accelerator, instant of photography-light flash, etc. Thus one has a convenient means of recording the relative times of the events.

ACKNOWLEDGMENTS

We wish to thank Professor Luis W. Alvarez for his interest in and sponsorship of this development. During some of the work one of us (W. L.) was aided considerably by electronics consulting with Vern Ogren.

This work was done under the auspices of the U. S. Atomic Energy Commission.

REFERENCES

1. Douglas Parmentier, Jr., and Arnold J. Schwemin, "Liquid-Hydrogen Bubble Chambers,, University of California Radiation Laboratory Report No. UCRL-2923, March 15, 1955. (This report contains further references.)

2. Harry Cline Dittler and Thomas Frank Gerecke, "Liquid-Hydrogen Bubble Chambers," (M.S. thesis), University of California Radiation Laboratory Report No. UCRL-2985, May 10, 1955. (This report contains a bibliography.)

3. Taft Wrathall, "Miniature Pressure Cells," Instruments 26, 736.

4. Linlor and Kerns, Pat. Application S-13, 216 (RL-1672).